The effect of nanoparticles on the thermal conductivity of crystalline thin films at low temperatures

Kamal M. Katika and Laurent Pilon[a)]
Mechanical and Aerospace Engineering Department, Henry Samueli School of Engineering and Applied Science, University of California Los Angeles, Los Angeles, California 90095, USA

(Received 15 August 2007; accepted 30 March 2008; published online 9 June 2008)

This study is concerned with the prediction of the effective thermal conductivity of nanocomposite thin films consisting of nanoparticles randomly distributed in a solid matrix. Crystalline sodium chloride with embedded monodisperse silver nanoparticles is investigated as a case study for thin films where phonons are the main heat carriers. To the best of our knowledge, the equation for phonon radiative transfer is solved for the first time, with an exact scattering transport cross section of the nanoparticles as a function of frequency which was obtained from the literature. The one-dimensional equation for phonon radiative transfer based on the isotropic scaling approximation is solved on a spectral basis using the discrete ordinates method to predict the temperature profile and the heat flux across the nanocomposite thin films. The thermal conductivity is retrieved at temperatures where the effects of Umklapp and normal processes can be neglected and scattering by the particles on phonon transport dominates. The method of solution and closure laws were validated with experimental data of thermal conductivity for bulk samples at 2.53, 5.94, and 10.56 K. The effects of the film thickness (1 μm to 2.5 cm), nanoparticle diameter (5 to 100 nm) and volume fraction (0.0001 to 0.2) on the thermal conductivity of the nanocomposite thin film are investigated. The results indicate that the thermal conductivity decreases with decreasing particle radius as well as with increasing particle concentration. Finally, a dimensional analysis revealed a power-law relationship between the dimensionless thermal conductivity and a dimensionless length of the order of the *acoustic* thickness of the medium. These results can be used to design nanocomposite thin films for various low-temperature thermal applications by choosing optimal nanoparticle radius and volume fraction, and film thickness. © *2008 American Institute of Physics*. [DOI: 10.1063/1.2937208]

I. INTRODUCTION

Nanocomposite materials can be described as materials consisting of embedded nanoparticles or nanopores in a solid matrix. They are considered for various applications as their properties can be tuned by varying the particle material, shape, size, and concentration. For example, bismuth nanowires in alumina nanocomposite materials have been used in thermoelectric applications to increase the thermoelectric figure of merit by increasing their electrical conductivity and reducing their thermal conductivity.[1] Nanocomposite materials have also been proposed for thermal interface materials whose properties can be tuned by varying the particle size and concentration.[2] Nanocomposite materials can also be used in low-temperature applications such as insulating materials in spacecraft and superconducting magnet devices.[3] In these applications, it is necessary to quantitatively assess the effect of nanoparticle radius and concentration on the thermal conductivity of nanocomposite materials.

Various experimental studies have been carried out to investigate the effect of nanoparticles on the thermal conductivity of various materials. Walton and Lee[4,5] reported that the thermal conductivity of bulk sodium chloride crystals decreases with increasing colloidal silver nanoparticle radius and concentration at low temperatures between 0.2 and 3 K. More recently, Kim *et al.*[6] reduced the thermal conductivity of $In_{0.53}Ga_{0.47}As$ below the alloy limit by adding ErAs nanoparticles ranging from 1 to 4 nm in diameter between 100 and 600 K. The alloy limit is the lowest thermal conductivity of crystalline solids that can be achieved by the scattering of phonons by atomic substitutions. Brochin *et al.*[7] also studied the effect of nanometer-sized silica inclusions on the thermal properties of bulk bismuth samples and observed a significant reduction in their thermal conductivity at temperatures ranging from 50 to 300 K.

Several authors have also reported numerical simulations of thermal conductivity of nanocomposite materials. For example, Yang and Chen[8] computed the thermal conductivity of periodic two-dimensional (2D) nanocomposites with square silicon nanowires in germanium, and studied the effect of the nanowire width and volumetric fraction at room temperature. They modeled the system as discrete units of silicon nanowires and germanium and solved the Boltzmann transport equation (BTE) in 2D on a gray basis separately for each medium. They considered a unit cell of an infinite array of silicon nanowires of widths 10 and 268 nm embedded in germanium with volume fractions ranging from 0.15 to 0.85. They concluded that the thermal conductivity of these nanocomposites decreases with decreasing the wire width at a

[a)]Author to whom correspondence should be addressed. Telephone: +1 (310)-206-5598; FAX: +1 (310)-206-2302. Electronic mail: pilon@seas.ucla.edu.

constant silicon volume fraction of 0.2. Jeng *et al.*[9] also considered a unit cell of an infinite array of silicon nanowires in germanium and used the Monte Carlo method to simulate phonon transport in 2D on a gray basis. They considered wires of square cross section and width ranging from 10 to 200 nm and volume fraction ranging from 0.1 to 0.4. They showed that the thermal conductivity of nanocomposites can be below the alloy limit.

Theoretical studies of the effect of nanoparticles on thermal conductivity were also reported by Prasher and coworkers. Prasher[10] computed the effective thermal conductivity of two-dimensional nanoporous and microporous materials made from aligned cylindrical pores using a ballistic-diffusive effective medium model. The author used a "view factor" approach on a gray basis, as in radiative heat transfer,[11] and computed the heat flux in a unit cell of a cylindrical nanopore in silicon. The author showed that the model compared very well with experimental data for 2.3 and 10.9 μm diameter pores and volume fractions of 0.233 and 0.26 at temperatures ranging from 20 to 300 K.[12] Prasher and Sinha[13] also used an approximate analytical solution of the BTE for phonon transport in 2D for a unit cell of a nanocomposite material consisting of nanowires in a host matrix. The analytical solution was used to predict the thermal conductivity of silicon-germanium nanocomposites with silicon wires of diameters 50 and 150 nm at volume fractions ranging from 0.1 to 0.8 at room temperature. The authors found a good agreement with experimental data reported in Ref. 1.

While several theoretical studies have investigated the effect of nanoparticles on the thermal conductivity of the matrix, they were all based on approximations of the BTE. For example, most of them treated phonon transport on a gray basis or considered "unit-cell" approaches to model phonon transfer in nanocomposite materials.[8–10] However, the gray approximation is inappropriate as the phonon relaxation times due to phonon scattering on nanoparticles and nanowires are strongly dependent on phonon frequency. In this study, the BTE is solved numerically on a spectral basis with accurate scattering properties to compute the thermal conductivity of a thin film of dielectric material with embedded nanoparticles. Sodium chloride crystals containing silver colloids are considered for simulations as a case study. To the best of our knowledge, this represents the first effort to use an accurate scattering transport cross section to solve the generalized equation for phonon radiative transfer on a spectral basis for a wide variety of particle sizes, concentrations, and film thicknesses.

II. THERMAL CONDUCTIVITY OF SODIUM CHLORIDE THIN FILMS WITH COLLOIDAL SILVER PARTICLES

A. Introduction

The thermal conductivity $k(T)$ of a bulk crystalline solid at temperature T where phonons are the dominant heat carriers can be expressed as[4]

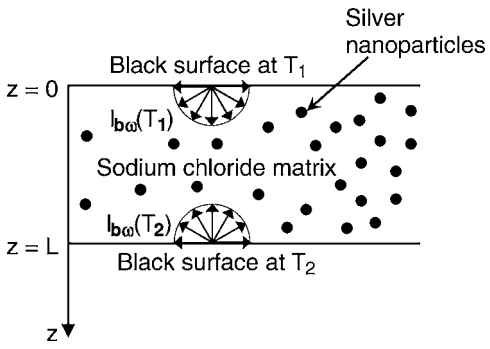

FIG. 1. A schematic of the geometry of the NaCl thin films used in the computations.

$$k(T) = \frac{k_B}{2\pi^2 v}\left(\frac{k_B T}{\hbar}\right)^3 \int_0^{\theta_D/T} \tau(x,T)\frac{x^4 e^x}{(e^x-1)^2}dx, \tag{1}$$

where k_B is the Boltzmann's constant, $\hbar$ is the Planck's constant divided by 2π, v is the average sound velocity in the material, θ_D is the Debye temperature, and τ is the relaxation time for phonon scattering on particles, boundaries, or on other phonons. The variable x is related to the phonon frequency ω and is equal to $\hbar\omega/k_B T$. Assuming that the different phonon scattering processes are independent from one another, the total relaxation time $\tau(x,T)$ can be expressed using Mathiessen's rule,[14]

$$1/\tau = 1/\tau_U + 1/\tau_N + 1/\tau_b + 1/\tau_p, \tag{2}$$

where the relaxation times τ_U, τ_N, τ_b, and τ_p are due to (1) Umklapp processes; (2) normal processes; (3) boundary scattering; and (4) particle scattering, respectively. It should be noted that τ_U, τ_N, and τ_p depend on the phonon frequency ω, and therefore on x. The main assumptions in deriving Eq. (1) are[15] (i) phonons are the only heat carriers; (ii) the Debye model is assumed to be valid, i.e., the phonons have a constant group velocity and cannot have a frequency greater than the Debye frequency ω_D; (iii) polarization effects are negligible and all three phonon polarizations are treated identically; (iv) optical phonons do not contribute to heat conduction due to their small group velocities; (v) the phase of the phonons is not accounted for, thus neglecting interference effects; and (vi) the scattering mechanisms are independent and the single-mode relaxation time approximation is used to replace the scattering term in the BTE; (vii) thermal expansion is neglected; and (viii) the medium is isotropic.

B. Analysis

Let us consider a sodium chloride (NaCl) thin film of thickness L containing randomly distributed monodisperse colloidal silver (Ag) nanoparticles as shown in Fig. 1. This particular system was chosen because the scattering coefficient of Ag nanoparticles in NaCl has been reported in the literature.[5] In addition, the thermal conductivity of bulk NaCl with Ag nanoparticles was measured at temperatures ranging from 0.2 to 3 K,[4] and at temperatures ranging from 1 to 100 K.[16] Walton[4] was also able to theoretically predict the thermal conductivity of the NaCl crystals with Ag nanoparticles from Eq. (1) by using a relaxation time given by $\tau=[v(B$

$+nC_{T,\omega})]^{-1}$, where B is the reciprocal of the boundary scattering length, n is the number of colloidal particles per unit volume, and $C_{T,\omega}$ is the transport cross section of a single colloidal particle. Note that the relaxation time due to boundary scattering τ_b is equal to $1/vB$, while that due to particle scattering, τ_p is given by $1/vnC_{T,\omega}$. Moreover, Umklapp and normal processes are not accounted for due to the low temperatures considered, at which τ_U, $\tau_N \gg \tau_b (=1/vB)$ and τ_U, $\tau_N \gg \tau_p (=1/unC_{T,\omega})$. Similarly, in the present study, the thermal conductivity at only low temperatures are studied to isolate the effect of nanoparticles and to neglect Umklapp and normal processes. This assumption is not valid for temperatures greater than temperatures around 10 K for NaCl with Ag colloidal particles. Finally, at temperature T much smaller than the Debye temperature θ_D, the upper limit θ_D/T of the integral in Eq. (1) can be treated as infinity.

Unfortunately, Eq. (1) is valid only for dielectric bulk samples whose thickness is much larger than the mean-free path of the heat carriers. In fact, it is an approximate solution to the BTE for phonons for cases when phonon transport is diffuse, i.e., when Fourier's law applies.[17] On the other hand, in order to compute the thermal conductivity of thin films whose thickness is comparable to the mean-free path of the phonons, one must solve the BTE.[17]

Majumdar[17] showed that the BTE for phonons can be rewritten in terms of the so-called phonon radiation intensity I_ω, defined as

$$I_\omega(\vec{r},\vec{s},t) = \frac{1}{4\pi}\sum_{p=1}^{3} \hbar\omega v(\vec{s}) f(\vec{r},\vec{s},p,t) D(\omega,p), \tag{3}$$

where $f(\vec{r},\vec{s},p,t)$ is the phonon distribution function and depends on particle position $\vec{r}$, polarization p, and time t. The unit vector in the direction of propagation of the phonons is $\vec{s}$, and $D(\omega,p)$ is the phonon density of states per unit volume for each one of the three phonon polarizations p. Note that the phonon velocity v can be also a function of phonon frequency ω. Then, if one makes the same assumptions as those listed in Sec. II A, the equation for phonon radiative transfer can be derived from the BTE and written as

$$\frac{\partial I_\omega}{\partial t} + (\vec{v}\cdot\nabla) I_\omega = \left(\frac{\partial I_\omega}{\partial t}\right)_{\text{scat}} \tag{4}$$

More recently, Prasher[18] proposed the generalized equation for phonon radiative transfer (GEPRT),

$$\frac{1}{v}\frac{\partial I_\omega}{\partial t} + (\vec{s}\cdot\nabla) I_\omega = K_{b,\omega}(I_\omega^0 - I_\omega) - K_{p,\omega} I_\omega + \frac{K_{p,\omega}}{4\pi}\int_{4\pi} I_\omega(\vec{s}_i)\Phi_{p,\omega}(\vec{s}_i,\vec{s})\mathrm{d}\Omega_i, \tag{5}$$

where the equilibrium intensity is denoted by I_ω^0 and defined as

$$I_\omega^0 = \frac{1}{4\pi}\int_{4\pi} I_\omega(\vec{s}_i)\mathrm{d}\Omega_i. \tag{6}$$

A clear correspondence can be seen between the terms of the radiative transfer equation[11] and those of the GEPRT. As in the GEPRT, I_ω represents the phonon intensity in a unit solid angle in the direction $\vec{s}$. The scattering coefficients for boundary and particle scattering are denoted by $K_{b,\omega}$ and $K_{p,\omega}$ and are equal to $1/v\tau_b = B$ and $1/v\tau_p$, respectively.

The first term on the right-hand side of Eq. (5) corresponds to the boundary scattering process. The second term on the right-hand side corresponds to attenuation of the intensity due to elastic scattering of phonons by the colloidal particles, and is denoted by the subscript p in the scattering coefficients. The last term corresponds to an augmentation of phonon radiation due to in-scattering on particles caused by multiple scattering. The scattering phase function $\Phi_{p,\omega}(\vec{s}_i,\vec{s})$ represents the probability that a phonon propagating in the solid angle $\mathrm{d}\Omega_i$ around direction $\vec{s}_i$ will be scattered by a particle into the solid angle $\mathrm{d}\Omega$ around the direction $\vec{s}$. In the case of isotropic phonon scattering, $\Phi_{p,\omega}(\vec{s}_i,\vec{s}) = 1$.

Thus, the EPRT is a particular case of the GEPRT when elastic scattering is isotropic.[18] Note also that Eq. (5) is valid for homogeneous and isotropic media where independent scattering prevails. Independent scattering occurs when the scattering by a particle is not influenced by the presence of a neighboring particle in contrast to dependent scattering.[19]

Note that boundary scattering predominates at very low temperatures in the absence of nanoparticles.[14] It has often been treated as a volumetric process similar to the other scattering processes as opposed to a boundary condition to the governing equation. This approximation was proposed by Callaway[14] for low-temperature applications. It has been extended by Holland[20] to account for polarization and heat conduction by both transverse and longitudinal phonons using their respective phonon dispersion spectrum. A correction factor can be introduced to account for surface roughness and possible edge effects.[20,21] However, the expression for the correction factor leads to the same thermal conductivity at low temperature. Holland[20] concluded that "…*at low temperature in the Debye region, two-mode conduction can be adequately represented by considering one average phonon.*" In addition, he found a good agreement between his model and Callaway's simpler model "…*in the impurity scattering and boundary scattering regions*." Note also that Callaway's model has been used successfully for various materials at low temperatures. These arguments justify the assumptions made in the present study, which is also concerned with low temperatures.

In the present study, a slightly different form of the GEPRT is used. The scattering term in the GEPRT is simplified using the equivalent isotropic scattering formulation as suggested in the literature.[4,22] The isotropic formulation consists of replacing the anisotropic scattering coefficient $K_{p,\omega}$ by an equivalent isotropic transport scattering coefficient, $K_{pT,\omega}$.[22] Then, the GEPRT can be written as

$$\frac{1}{v}\frac{\partial I_\omega}{\partial t} + (\vec{s}\cdot\nabla) I_\omega = K_{b,\omega}(I_\omega^0 - I_\omega) - K_{pT,\omega} I_\omega + \frac{K_{pT,\omega}}{4\pi}\int_{4\pi} I_\omega(\vec{s}_i)\mathrm{d}\Omega_i. \tag{7}$$

Moreover, substituting Eq. (6) in Eq. (7) yields

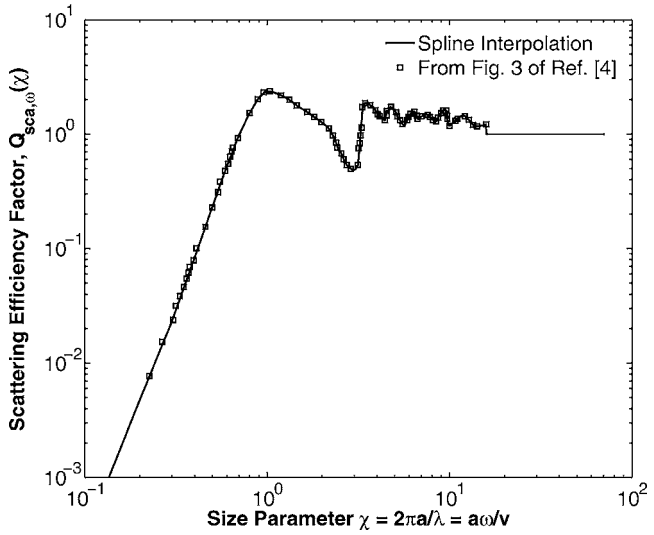

FIG. 2. The scattering efficiency factor $Q_{sca,\omega}$ of Ag colloidal nanoparticles in crystalline NaCl as a function of size parameter χ (Ref. 4).

$$\frac{1}{v}\frac{\partial I_\omega}{\partial t} + (\vec{s}\cdot\nabla)I_\omega = (K_{b,\omega} + K_{pT,\omega})(I_\omega^0 - I_\omega). \tag{8}$$

Finally, $K_{pT,\omega}$ is the transport scattering coefficient and is equal to $nC_{T,\omega}$.[4] The particle concentration is denoted by n, while the transport cross section of a single spherical Ag nanoparticle in NaCl crystals is denoted by $C_{T,\omega}(\chi)$ and depends only on χ, the particle size parameter defined as $2\pi a/\lambda(=a\omega/v)$, where a is the particle radius and λ is the phonon wavelength equal to $2\pi v/\omega$. Thus, Eq. (8) simplifies to

$$\frac{\partial I_\omega}{\partial t} + v(\vec{s}\cdot\nabla)I_\omega = v(B + nC_{T,\omega})(I_\omega^0 - I_\omega). \tag{9}$$

The parameter B was obtained from Ref. 16 and is equal to 181.82 m^{-1}. The transport cross section $C_{T,\omega}(\chi)$ of spherical Ag nanoparticles in NaCl crystals as a function of particle size parameter was computed by Walton and Lee[5] using a partial wave analysis. It was reported for particles of radius 6.4 nm (Fig. 3 of Ref. 4) as a function of the size parameter.

The scattering efficiency factor $Q_{sca,\omega}(\chi)$, defined as $C_{T,\omega}/\pi a^2$,[11] is then used to compute the transport cross section of particles of different sizes. Figure 2 shows the scattering efficiency factor of Ag nanoparticles in NaCl crystals as a function of the size parameter χ obtained by a spline interpolation through the discrete points obtained from Ref. 4. Note that the scattering efficiency factor tends to 1.0 for large values of χ.[11] Here, $Q_{sca,\omega}(\chi)$ is set to 1.0 for χ greater than 20. In addition, the Debye temperature and the speed of sound in NaCl were taken as 321 K (Ref. 23) and 3800 m/s,[16] respectively.

Finally, the following boundary conditions corresponding to black thermalizing boundaries are imposed:[15]

$$I_\omega(z=0,\theta) = I_{b\omega}(T_1) = \frac{3\hbar\omega^3}{8\pi^3 v^2(e^{\hbar\omega/k_B T_1} - 1)}$$

$$\text{for} \quad 0 \le \theta \le \pi/2, \tag{10}$$

and

$$I_\omega(z=L,\theta) = I_{b\omega}(T_2) = \frac{3\hbar\omega^3}{8\pi^3 v^2(e^{\hbar\omega/k_B T_2} - 1)}$$

$$\text{for} \quad \pi/2 \le \theta \le \pi, \tag{11}$$

where T_1 and T_2 are the temperatures at locations $z=0$ and $z=L$ as shown in Fig. 1.

The phonon spectral intensity I_ω, the solution of Eqs. (9)–(11), is then used to compute the temperature T and heat flux q'' in the z-direction at all locations according to[17]

$$T^4(z) = \frac{\pi}{2\sigma}\int_0^{\omega_D}\int_0^{\pi} I_\omega(z,\theta)\sin\theta d\theta d\omega \tag{12}$$

and

$$q''(z) = \int_0^{\omega_D}\int_0^{\pi} I_\omega(z,\theta)\sin\theta\cos\theta d\theta d\omega, \tag{13}$$

where θ is the polar angle and σ is the Stefan-Boltzmann constant for phonons and is equal to $\pi^2 k_B^4/40\hbar^3 v^2$. Finally, the dimensionless temperature and the dimensionless length are defined as $T^*=(T^4-T_2^4)/(T_1^4-T_2^4)$ and $z^*=z/L$, respectively.

Then, the expression for the effective thermal conductivity can be obtained in the following manner. The dimensionless temperature T^* is linearly dependent on the dimensionless length z^*, so that[11]

$$\frac{T^4 - T_2^4}{T_1^4 - T_2^4} = m\frac{z}{L} + c, \tag{14}$$

where m and c are constants for a given particle concentration, particle radius, and film thickness. Differentiating this equation with respect to z yields

$$\frac{4T^3}{T_1^4 - T_2^4}\frac{dT}{dz} = m/L. \tag{15}$$

Recognizing that $q''=-k(dT/dz)$, where k is an effective thermal conductivity,[17] and after rearrangement, the following equation for thermal conductivity is obtained:

$$k(T) = -\frac{4T^3 L q''}{m(T_1^4 - T_2^4)}. \tag{16}$$

The temperature T and heat flux q'' at which the thermal conductivity is computed can be chosen at any location within the thin film. In this study, both T and q'' were computed at the center of the thin film as the temperature at this location was the same for all values of particle radius, concentration, and film thickness for a given set of T_1 and T_2, i.e., $T^*=0.5$ at $z^*=0.5$. In all cases, T_1 and T_2 were equal to 3 and 1 K, respectively, unless otherwise mentioned.

C. Method of solution

The discrete ordinates method[11] is employed to solve the GEPRT for isotropic scattering [Eq. (9)] for a thin film of thickness L. Under one-dimensional steady-state conditions, the equation can be discretized as

$$\cos\theta_l \frac{I_{\omega,k}^{m+1} - I_{\omega,k-1}^{m+1}}{\Delta z} = (B + nC_{T,\omega})(I_{\omega,k}^{0m} - I_{\omega,k}^{m+1}), \quad 0 \le \theta \le \pi/2, \quad 2 \le k \le N_z, \tag{17}$$

$$\cos\theta_l \frac{I_{\omega,k+1}^{m+1} - I_{\omega,k}^{m+1}}{\Delta z} = (B + nC_{T,\omega})(I_{\omega,k}^{0m} - I_{\omega,k}^{m+1}) \quad \pi/2 \le \theta \le \pi, \quad 1 \le k \le N_z - 1, \tag{18}$$

where N_z is the number of discrete points in the z-direction, k is the index for the discrete location along the z-direction, l is the index for the discrete polar angle, and m is the iteration step. Moreover, the polar angle θ and the angular frequency ω from 0 to ω_D were discretized into N_θ and N_ω angles and frequencies, respectively. Equations (17) and (18), along with all integrals over the polar angle θ encountered in computing the equilibrium intensity I_ω^0, temperature, and heat flux are evaluated using an S_8 Gaussian quadrature having four angles per quadrant.[11] A higher quadrature was not needed as the intensity I_ω at a given location was independent of the polar angle θ due to the isotropic scaling approximation and diffuse boundary conditions.

Equations (17) and (18) are then solved iteratively until a converged solution is obtained. The iterations were assumed to be converged when the change in heat flux at all locations from one iteration to the next was less than 0.01%. The numerical convergence was tested by varying N_z and N_ω. The number of points N_z required for numerical convergence ranged from 21 to 41 depending on the particle volume fraction and the particle radius, while the number of angular frequencies N_ω to achieve convergence was 91 for all cases. It was assumed that numerical convergence was achieved when the variation in the heat flux at a given location was less than 0.1% when N_z or N_ω was doubled.

D. Validation

For validation purposes, the code was used to predict the temperature profile in a bulk NaCl sample with embedded Ag nanoparticles of radius $a=6.4$ nm at a concentration of $n=1.5\times10^{20}/\mathrm{m}^3$. This concentration was chosen to compare the computed thermal conductivity with that obtained experimentally by Walton[4] and Worlock[16] for NaCl samples of unknown thickness. The thermal conductivity of bulk NaCl at temperature $T=2.53$ K was computed by solving Eqs. (9)–(16) for an arbitrary thickness of 2.5 cm for which Fourier's law applied. The result falls within 8% of the thermal conductivity predicted by Eq. (1) and within 1.7% of the experimental value reported by Walton[4] for the same particle radius and concentration. Finally, the thermal conductivity was computed at temperatures of 5.94 and 10.56 K and compared with experimental data obtained by Worlock[16] for the same system. The relative differences between the experimental data and numerical predictions at these two temperatures were 6.0 and 4.8%, respectively. These results for 2.53, 5.94, and 10.56 K are very good, given the approximations made and the uncertainty in the closure laws. They validate the code which can now be used to compute the thermal conductivity of nanocomposite thin films. The predictions of the thermal conductivity as a function of film thickness, particle radius, and concentration are reported in the following section.

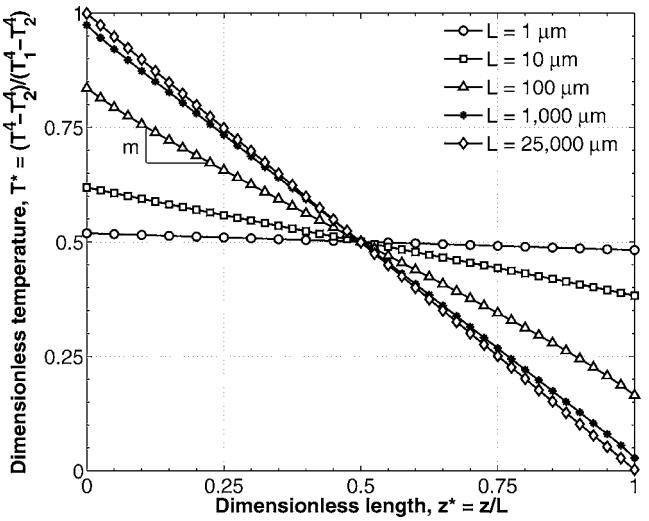

FIG. 3. Dimensionless temperature T^* as a function of dimensionless length z^* in NaCl films of varying thickness containing Ag nanoparticles with $a=6.4$ nm, $\phi=1.65\times10^{-4}$, $T_1=3$ K, and $T_2=1$ K.

III. RESULTS AND DISCUSSION

A. Effect of film thickness

The thermal conductivity of NaCl nanocomposite thin films was computed at 2.53 K for five values of thickness L, namely, 1, 10, 100, 1000, and 25 000 μm. All five films contained spherical colloidal Ag particles of radius a equal to 6.4 nm at a concentration n of $1.5\times10^{20}/\mathrm{m}^3$, corresponding to a volume fraction ϕ of $\phi=1.65\times10^{-4}$, where $\phi=\frac{4}{3}\pi a^3 n$. The values of a, n, and ϕ were chosen to compare the numerical results with experimental data reported by Walton.[4]

Figure 3 shows the profile of the dimensionless temperature T^* as a function of dimensionless length z^* for the five thicknesses considered. The dimensionless temperature T^* varies from a ballistic regime to a diffusive regime with increasing thickness, as observed by Majumdar.[17] Equation (16) is then used to compute the thermal conductivity of these films from the slope m of the lines in Fig. 3.

Figure 4 shows the evolution of thermal conductivity at 2.53 K as a function of film thickness L for two different particle volume fractions ϕ of $\phi=1.65\times10^{-4}$ and 0.001. It indicates that the thermal conductivity starts to plateau for film thicknesses larger than 1000 μm, indicating that the thermal conductivity of the film has almost approached that of the bulk. Moreover, the thermal conductivity also decreases with increasing the particle volume fraction for a given film thickness. Figure 4 also shows the thermal con-

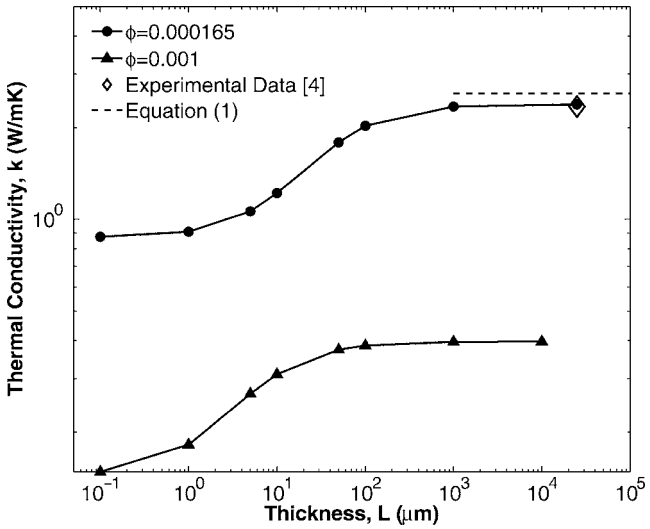

FIG. 4. Thermal conductivity of NaCl thin films containing Ag nanoparticles of radius 6.4 nm as a function of film thickness L and volume fraction ϕ at 2.53 K obtained from numerical simulations along with reported experimental values.

ductivity value of a bulk sample at 2.53 K measured experimentally by Walton[4] at 2.35 W/mK. As mentioned earlier, the experimental value of thermal conductivity is about 1.7% smaller than the value computed in the present study using the GEPRT.

B. Effect of particle radius

The thermal conductivity at 2.53 K of a 100 μm NaCl thin film was also computed as a function of Ag particle radius a while the volume fraction ϕ of the nanoparticles was kept constant at $\phi=1.65\times10^{-4}$. Figure 5 shows the profile of the dimensionless temperature T^* as a function of dimensionless length z^* for particle radius ranging from 5 nm to 1 μm. It indicates that phonon transport tends toward the ballistic regime as the particle radius increases. This is due to the fact that the *acoustic* thickness $K_{e,\omega}L$, expressed as

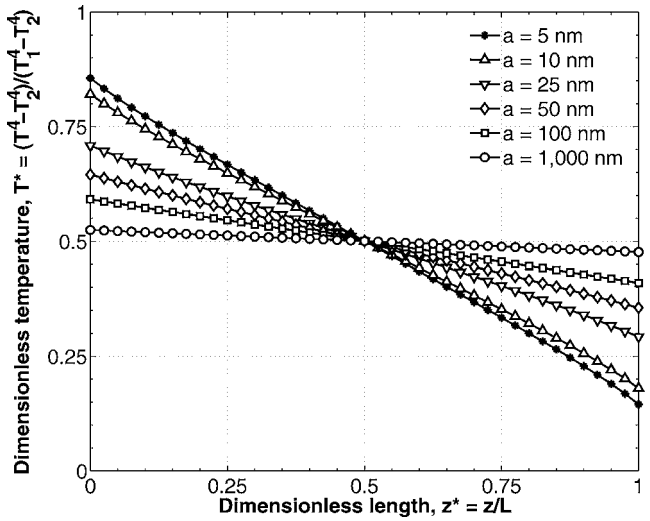

FIG. 5. Dimensionless temperature T^* as a function of dimensionless length z^* in a 100 μm NaCl film with colloidal Ag nanoparticles of various radii a with $\phi=1.65\times10^{-4}$, $T_1=3$ K, and $T_2=1$ K.

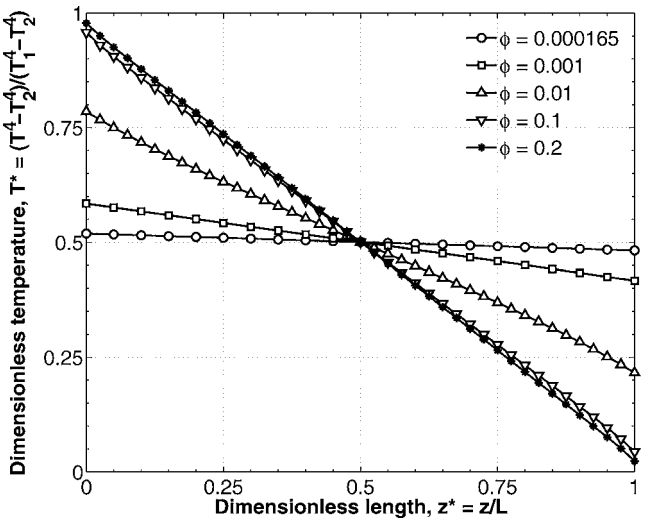

FIG. 6. Dimensionless temperature T^* as a function of dimensionless z^* length in a 1 μm NaCl film with colloidal Ag nanoparticles of various volume fractions with $a=6.4$ nm, $T_1=3$ K, and $T_2=1$ K.

$$K_{e,\omega}L=(nC_{T,\omega}+B)L=\left(\frac{3\phi}{4a}Q_{\mathrm{sca},\omega}+B\right)L, \tag{19}$$

decreases with increasing particle radius a for a given particle volume fraction ϕ. Note that $Q_{\mathrm{sca},\omega}$ also increases with increasing the particle radius but not sufficiently to compensate for the increase in particle radius in the denominator of $(3\phi/4a)Q_{\mathrm{sca},\omega}$.

C. Effect of particle volume fraction

The thermal conductivity at 2.53 K of a 1 μm thin composite NaCl film was computed for different particle volume fractions ϕ ranging from $\phi=1.65\times10^{-4}$ to 0.2. Note that independent scattering is still assumed in spite of the high concentrations of the particles. For particle concentrations greater than 0.01 and size parameter less than 0.4, scattering is always dependent in the case of photon radiative transfer.[19] Since we encounter these concentrations and size parameters in our simulations, albeit for phonon radiative transfer, we might expect dependent scattering effects.[24] The application of results in photon transport to phonon radiation transfer as suggested by Prasher[24] remains speculative but is used in this study as a qualitative criterion.

The particle radius a was uniform and constant at 6.4 nm. Figure 6 shows the dimensionless temperature profile as a function of the dimensionless length for these various particle concentrations. Phonon transport changed from a ballistic to a diffuse regime with increasing the particle volume fraction. This is due to a decrease in the relaxation time with increasing the volume fraction ϕ and a corresponding increase in the *acoustic* thickness for a given particle radius. Note also that the dimensionless temperature profile for particle volume fractions of 0.1 and 0.2 approaches that of a thick slab even though the sample is only 1 μm thick. Typically, phonon transport at this temperature is ballistic for a film thickness of 1 μm in the absence of nanoparticles.

Moreover, an attempt was made to analyze the thermal conductivity of the thin films in terms of dimensionless

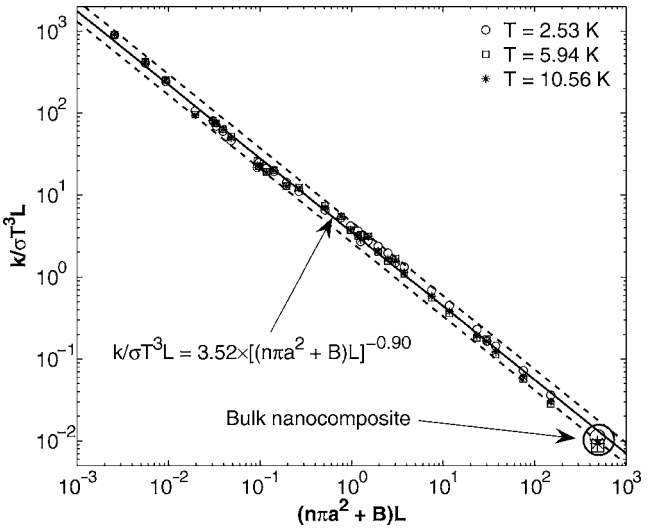

FIG. 7. The dimensionless quantity $k/\sigma T^3 L$ of NaCl thin films containing Ag nanoparticles of various sizes and concentrations as a function of dimensionless parameter $(n\pi a^2+B)L$ at various temperatures.

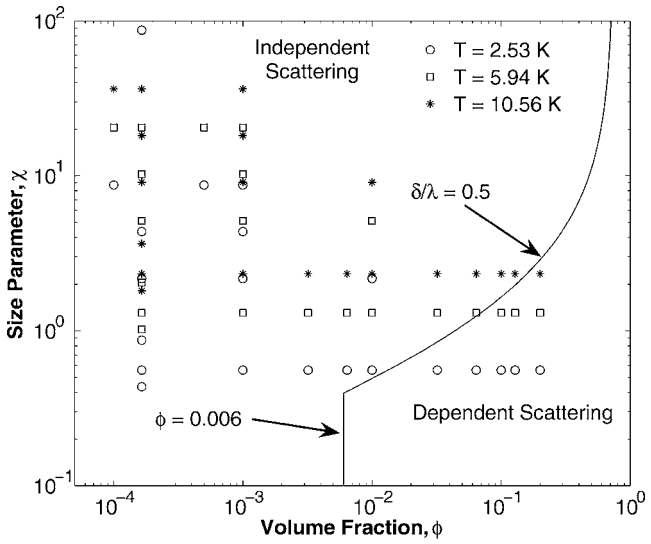

FIG. 8. Parameters explored for numerical simulations performed at three different temperatures on the independent and dependent scattering regime map (Ref. 19).

quantities. After dividing by the Stefan-Boltzmann constant for phonons in NaCl denoted by σ, Eq. (16) can be rewritten as

$$\frac{k}{\sigma T^3 L} = -\frac{4q''}{m\sigma(T_1^4 - T_2^4)}. \tag{20}$$

The quantity $q''/\sigma(T_1^4-T_2^4)$ is the dimensionless phonon radiative heat flux, akin to the dimensionless radiative heat flux encountered in radiative heat transfer.[11] In radiative heat transfer, the dimensionless heat flux depends only on the optical thickness of the medium.[11] By analogy, it is anticipated that the dimensionless phonon radiative heat flux is also solely dependent on the acoustic thickness of the medium $K_{e,\omega}L$ given by Eq. (19). Moreover, it was also observed in the numerical simulations that the slope m is dependent only on $K_{e,\omega}L$. Therefore, $k/\sigma T^3 L$ should depend only on the acoustic thickness. Figure 7 shows a plot of $k/\sigma T^3 L$ as a function of the dimensionless quantity $(n\pi a^2+B)L$ which is of the same order of magnitude as the acoustic thickness $K_{e,\omega}L$. Figure 7 indicates that $k/\sigma T^3 L$ is dependent only on $(n\pi a^2+B)L$ and falls on a straight line when plotted on a log-log scale. This indicates a power-law relationship given by

$$\frac{k}{\sigma T^3 L} = 3.52 \times [(n\pi a^2 + B)L]^{-0.90}, \tag{21}$$

for $k/\sigma T^3 L$ ranging from 0.01 to 1000 and $(n\pi a^2+B)L$ ranging from 0.001 and 1000. The square of the correlation coefficient R^2 was 0.9969, indicating a very good fit, particularly for such a wide range of values. Figure 7 also shows in dash lines the 95% confidence intervals for this power-law relationship.

Finally, the validity of the independent scattering assumption is checked by plotting the size parameter χ in the simulations against the particle volume fraction ϕ of all the simulations performed to produce Fig. 7 as shown in Fig. 8. An average size parameter $\chi=2\pi a/\lambda$ is determined by calculating a characteristic wavelength for each temperature defined as $\lambda=hv/k_B T$ and as used by Dames and Chen.[25] While a majority of the simulations falls in the independent scattering regime, there are a few which violate the independent scattering assumption. In spite of this, the results of all these simulations still obey Eq. (21) very closely.

IV. CONCLUSIONS

The thermal conductivity of NaCl thin films with embedded monodisperse spherical Ag nanoparticles was computed as a function of various parameters: film thickness ranging from 1 μm to 2.5 cm, particle radius from 5 nm to 1 μm, particle volume fraction from 0.0002 to 0.2, and temperatures of 2.53, 5.94, and 10.56 K. The steady-state GEPRT was solved using the discrete ordinates method, with the scattering coefficient of the particles as a function of the phonon frequency obtained from the literature. It is assumed that independent scattering prevailed in spite of the high particle volume fractions involved in some cases. Umklapp and normal processes were neglected due to the low temperatures considered. The method of solution of the GEPRT and the closure laws were validated with experimental data for bulk samples at 2.53, 5.94, and 10.56 K. The thermal conductivity of the thin films increases with increasing film thickness and reaches the bulk value for a thickness of around 1000 μm at 2.53 K. The thermal conductivity also increased with increasing the particle radius for a given thickness and particle concentration. Moreover, the thermal conductivity decreased with increasing particle concentration for a fixed film thickness and particle radius. Finally, a dimensional analysis revealed a power-law relationship between the dimensionless thermal conductivity $k/\sigma T^3 L$ and the dimensionless quantity $(n\pi a^2+B)L$ which is of the order of the acoustic thickness of the nanocomposite film. This analysis can be used to choose a combination of nanoparticle radius and concentration to achieve the desired thermal conductivity and film thickness for low-temperature applications.

ACKNOWLEDGMENTS

This material is based upon work supported by the National Science Foundation under Grant No. CTS 0449429.

[1]G. Chen, M. S. Dresselhaus, G. Dresselhaus, J. P. Fleurial, and T. Caillat, Int. Mater. Rev. **48**, 45 (2003).
[2]S. A. Putnam, D. G. Cahill, B. J. Ash, and L. S. Schadler, J. Appl. Phys. **94**, 6785 (2003).
[3]Z. Wang, J. Lu, Y. Li, S. Fu, S. Jiang, and X. Zhao, Mater. Sci. Eng., B **123**, 216 (2005).
[4]D. Walton, Phys. Rev. **157**, 720 (1967).
[5]D. Walton and E. J. Lee, Phys. Rev. **157**, 724 (1967).
[6]W. Kim, J. Zide, A. Gossard, D. Klenov, S. Stemmer, A.Shakouri, and A. Majumdar, Phys. Rev. Lett. **96**, 045901 (2006).
[7]F. Brochin, B. Lenoir, X. Devaux, and H. Scherrer, "Thermoelectric properties of bismuth-silica nanocomposites," in 18th IEEE International Conference on Thermoelectrics, Baltimore, MD (1999), pp. 390–393.
[8]R. Yang and G. Chen, Phys. Rev. B **69**, 195316 (2004).
[9]M.-S. Jeng, R. Yang, and G. Chen, "Monte Carlo simulation of thermoelectric properties in nanocomposites," in 24th IEEE International Conference on Thermoelectrics, Clemson, SC (2005), pp. 21–26.
[10]R. Prasher, J. Appl. Phys. **100**, 064302 (2006).
[11]M. F. Modest, *Radiative Heat Transfer* (Academic Press, San Diego, CA, 2003).
[12]D. Song, "Phonon heat conduction in nano and micro-porous thin films," Ph.D. thesis, University of California, Los Angeles (2003).
[13]R. S. Prasher and S. Sinha, The Tenth Intersociety Conference on Thermal and Thermomechanical Phenomena in Electronics Systems ITHERM '06 (2006), http://ieeexplore.ieee.org/xpls/abs_all.jsp?arnumber=1645488.
[14]J. Callaway, Phys. Rev. **113**, 1046 (1959).
[15]L. Pilon and K. Katika, ASME J. Heat Transfer **126**, 735 (2004).
[16]J. M. Worlock, Phys. Rev. **147**, 636 (1966).
[17]A. Majumdar, ASME J. Heat Transfer **115**, 7 (1993).
[18]R. S. Prasher, Appl. Phys. Lett. **83**, 48 (2003).
[19]C. L. Tien and B. L. Drolen, "Thermal radiation in particulate media with dependent and independent scattering," in *Annual Review of Numerical Fluid Mechanics and Heat Transfer*, edited by T. C. Chawla (Hemisphere, New York, 1987), Vol. 1, pp. 1–32.
[20]M. G. Holland, Phys. Rev. **132**, 2461 (1963).
[21]M. Asheghi, M. N. Touzelbaev, Y. K. Leung, and S. S. Wong, ASME J. Heat Transfer **120**, 30 (1998).
[22]Z. Guo and S. Maruyama, Int. Commun. Heat Mass Transfer **26**, 997 (1999).
[23]Del Mar Ventures, Sodium chloride NaCl. http://www.sciner.com/Opticsland/NaCl.htm, last accessed 26 July 2007.
[24]R. Prasher, ASME J. Heat Transfer **128**, 627 (2006).
[25]C. Dames and G. Chen, J. Appl. Phys. **95**, 682 (2004).